Pergamon

PII: S0277–5387(97)00043–0

Polyhedron Vol. 16, No. 17, pp. 3033–3038, 1997

0277–5387/97 $17.00+0.00

Linkage isomerism in complexation of Cu^{II} with 7-[(2-methylthiophenyl)azo]-8-hydroxyquinoline-5-sulfonate

Longhe Piao, Fumiaki Kai,* Masaaki Hirohata, Izumi Moritake,
Yuka Nakano and Schuichi Era

Department of Chemistry, Faculty of Science, Kumamoto University, Kurokami, Kumamoto 860, Japan

(Received 27 August 1996)

Abstract—7-[(2-Methylthiophenyl)azo]-8-hydroxyquinoline-5-sulfonate (mtaq) coordinates to Cu^{II} with an S,N,O-donor site at $-\log[H^+] < 2.7_5$ and N,O-donor site of only 8-hydroxyquinoline fragment at $-\log[H^+] > 2.7_5$, indicating the linkage isomerism. The rate constant ($k_2 = (3.2\pm0.5)\times10^2\ mol^{-1}\ dm^3\ s^{-1}$) for the pathway $[Cu(H_2O)_6]^{2+} + H_2mtaq \rightarrow Cu(Hmtaq)^+$-S,N,O is larger than that ($k_1 = 5.7\pm0.4\ mol^{-1}\ dm^3\ s^{-1}$) for the pathway $[Cu(H_2O)_6]^{2+} + Hmtaq^- \rightarrow Cu(mtaq)$-N,O. For a comparison, a reaction of Cu^{II} with 2-[(2-methylthiophenyl)azo]-1-hydroxynaphthalene-4-sulfonate (mαtan), which should naturally coordinate by using an S,N,O-site, was also studied. The rate constant obtained ($k = (4.1\pm0.5)\times10^2\ mol^{-1}\ dm^3\ s^{-1}$) for the pathway $[Cu(H_2O)_6]^{2+} + Hm\alpha tan^- \rightarrow Cu(m\alpha tan)^+$-S,N,O is quite similar in magnitude to the above k_2, indicating the formation of the $Cu(Hmtaq)^+$-S,N,O at the lower $-\log[H^+]$ region. © 1997 Elsevier Science Ltd

Keywords: Cu^{II}-complex; S,N,O-ligand; linkage isomerism; complexation equilibrium; kinetics.

We have reported hitherto the coordination selectivities of many kinds of azo system multidentate ligands containing N and O atoms as donor sites toward various metal ions chosen from the viewpoint of their softness [1–12].

In this paper, the study was extended to a complexation of thioether system ligand, 7-[(2-methylthiophenyl)azo]-8-hydroxyquinoline-5-sulfonate ($Hmtaq^-$, Scheme 1), which was prepared for the first time, because of the tacit understanding that the sulfur donors influence characteristically the reactivity of metal centers [13]. The metal ion chosen was Cu^{II}, because copper has usually a large affinity for an S atom in various biological systems and displays differing chemical properties, presumably because of the different ligand environment.

It was found that mtaq reacts with Cu^{II} to form an S,N,O-tridentate complex at the lower $-\log[H^+]$ region and an N,O-bidentate complex at higher $-\log[H^+]$ region, respectively. That is, a linkage isomerism was observed in this complexation due to the $-\log[H^+]$ region studied. This paper describes an evidence of the linkage isomerism by the UV–vis and Raman spectroscopies, and the kinetics in detail.

EXPERIMENTAL

Preparation of ligands

The ligand mtaq was synthesized by the usual coupling reaction as follows: commercial (Aldrich) 2-methylthioaniline (2.78 g, 20 mmol) was diazotizated by the usual method [14]. To an aqueous solution of commercial (Tokyo Kasei) 8-hydroxyquinoline-5-sulfonate (2.25 g, 20 mmol) with sodium hydroxide, an aqueous solution containing diazotizated thioanisidine was added with stirring. A crude product was then obtained by acidification with dilute acetic acid (1:1) after stirring for *ca* 6 h at 5°C. The product was recrystallized from acidic aqueous solution containing hydrochloric acid, then dried *in vacuo*. Yield, 60%; m.pt (decomp.) > 300°C. Found: C, 40.6; H, 3.2; N, 8.9. Calc. for $C_{16}H_{12}N_3O_4S_2Na\cdot H_2O\cdot NaCl$: C, 40.6; H, 3.0; N, 8.9%. IR: 1393 cm^{-1} ($\nu_{N=N}$). ^1H NMR

---

*Author to whom correspondence should be addressed.

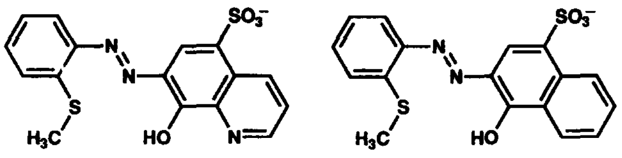

mtaq **mαtan**

Scheme 1. Chemical formulae of the new ligands.

[20% v/v $(CD_3)_2SO—D_2O$] : δ 2.40 (3H, s, CH_3), 7.24 (3H, m), 7.50 (1H, dd, $J = 8.50$, 4.25 Hz), 7.67 (1H, d, $J = 7.18$ Hz), 8.30 (1H, s), 8.58 (1H, dd, $J = 4.25$, 1.32 Hz), 8.77 (1H, dd, $J = 8.43$, 1.69 Hz).

To see a role of the N atom in the hydroxyquinoline ring of mtaq, 2-[(2-methylthiophenyl)azo]-1-hydroxynaphthalene-4-sulfonate (mαtan, Scheme 1) was also synthesized by a similar coupling method to mtaq and was recrystallized from an acidic aqueous solution. Yield, 66%, m.pt (decomp.) > 300°C. Found: C, 50.3; H, 3.2; N, 7.2. Calc. for $C_{17}H_{13}N_2O_4S_2Na \cdot 1/2H_2O$: C, 50.3; H, 3.5; N, 6.9%. IR: 1392 cm^{-1} ($\nu_{N=N}$). ^1H NMR (D_2O): δ 2.48 (3H, s, CH_3), 7.16–7.79 (6H, m, H-3′, H-4′, H-5′, H-6′, H-6 and H-7), 8.29–8.63 (2H, m, H-5 and H-8), 8.46 (1H, s, H-3).

Measurements

Raman spectra were recorded on a JASCO R-800 spectrometer equipped with an NEC GLG 3200 Ar^+ laser as an exciting light source. The excitation wavelength was 488.0 nm.

A corrected hydrogen ion concentration $[H^+]$ was calculated from the relation:

$$-\log[H^+] = pH_{meas} + \log f_{H^+},$$

in which pH_{meas} refers to a measured pH value by a pH meter and the activity coefficient f_{H^+} of 0.83 at 25°C was estimated [14].

All the other measurements are the same as those described elsewhere [11,12].

RESULTS AND DISCUSSION

Protonation constants of ligands

The fully protonated species H_2mtaq gives two dominant peaks at 18.4×10^3 cm^{-1}, corresponding to the $\pi^* \leftarrow \pi$ transition of the azo group [15] and around 20.9×10^3 cm^{-1} due to the quinoline ring [16]. Both of these absorption bands are shifted hypsochromically upon deprotonation. A protonation sequence of mtaq is considered to be at first from HO— in 8-hydroxyquinolinolate ($K_{(hqOH)}$), then from HN^+— in 8-hydroxyquinoline ($K_{(hqNH)}$) on the basis of a mutual comparison of these values and with those of analogous ligands [17]. The protonation constants, together with those for mαtan, obtained from the spectral changes in aqueous solution are listed in Table 1.

Table 1. Protonation constants[a] of ligands and stability constants of Cu^{II} complexes in log unit at $\mu = 0.1$ (KNO_3), 25.0±0.2°C

	mtaq	mαtan	Remark
$K_{(hqNH)}$	2.9_9		Quinoline
$K_{(hqOH)}$	7.5_4		Quinolinolate
$K_{(npOH)}$		8.1_2	Naphtholate
$\beta_{Cu(Hmtaq)\text{-}S,N,O}$	12.6_6		Low $-\log[H^+]$ region
$\beta_{Cu(mtaq)\text{-}N,O}$	19.7_8		High $-\log[H^+]$ region
$\beta_{Cu(m\alpha tan)\text{-}S,N,O}$		15.5_1	

[a] $K_{(hqNH)}$ (mol^{-1} dm^3) = $[H_2mtaq]/[Hmtaq^-][H^+]$, $K_{(hqOH)}$ (mol^{-1} dm^3) = $[Hmtaq^-]/[mtaq^{2-}][H^+]$ and $K_{(npOH)}$ (mol^{-1} dm^3) = $[Hm\alpha tan]/[m\alpha tan^-][H^+]$.

Electronic spectra of Cu^{II}*-mtaq and -mα tan complexes*

It is well-known that a comparison of absorption maxima by the $\pi^* \leftarrow \pi$ transition of the azo group in both free ligands and their metal complexes provides a deductive information whether an N atom in the azo group coordinates to metal ions or not [1,2,7].

Figure 1 depicts the electronic spectra of the free ligands and their Cu^{II} complexes. The absorption of the species H_2mtaq at 18.0×10^3 cm^{-1} (a) was scarcely, or slightly, shifted upon the Cu^{II}-mtaq complexation at $-\log[H^+]$ 2.4_5 (b). On the other hand, the absorption maximum of the spectrum for the Cu^{II}-mtaq complex at $-\log[H^+]$ 7.0_8 (c) is markedly shifted to 22.0×10^3 cm^{-1}.

The above spectral features were compared with those of mαtan and its Cu^{II} complex, because mαtan, as can be seen from the molecular structure, should coordinate naturally to an S,N,O site. As a result, the wavelength of the absorption maximum of the species $Hm\alpha tan^-$ at $-\log[H^+]$ 5.5_3 [(d), 19.2×10^3 cm^{-1}] was scarcely shifted compared with that of the Cu^{II} complex at $-\log[H^+]$ 6.9_1 [(e), 19.0×10^3 cm^{-1}]. This indicates that the coordination mode of the Cu^{II}-mtaq complex at lower $-\log[H^+]$ region resembles that for the complex Cu^{II}-mαtan; namely suggesting the S,N,O-coordination mode.

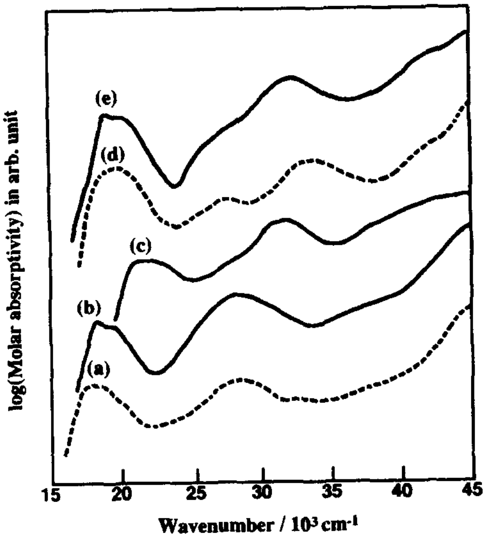

Fig. 1. Electronic spectra of ligands and their Cu^{II} complexes: (a) H_2mtaq at $-\log[H^+]$ 1.8_8; (b) Cu(Hmtaq)$^+$-S,NO,O at $-\log[H^+]$ 2.4_5; (c) Cu(mtaq)-N,O at $-\log[H^+]$ 7.9_3; (d) Hmαtan$^-$ at $-\log[H^+]$ 5.5_3; (e) Cu(mαtan)-N,O at $-\log[H^+]$ 6.9_1. [ligand] $= 2.00 \times 10^{-5}$ mol dm^{-3}, $[Cu^{II}] = 2.00 \times 10^{-4}$ mol dm^{-3}, $\mu = 10^{-1}$ mol dm^{-3} $NaClO_4$, 25.0 ± 0.5°C.

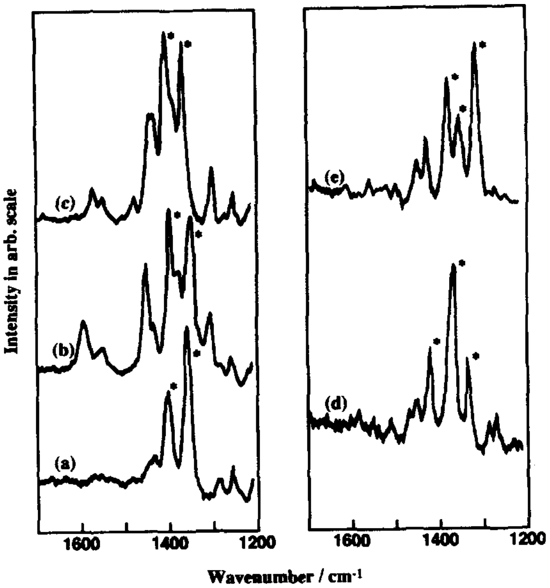

Fig. 2. Two series of absorption spectral changes of the Cu^{II}-mtaq complex in the $-\log[H^+]$ ranges 0–2.7_5 and 2.7_5–5.8_9. [mtaq] $= 2.00 \times 10^{-5}$ mol dm^{-3}, $[Cu^{II}] = 2.00 \times 10^{-4}$ mol dm^{-3}, $\mu = 10^{-1}$ mol dm^{-3} $NaClO_4$, 25.0 ± 0.5°C.

Resonance Raman spectra of the azo group

To confirm an estimation from the above electronic spectral measurements for the coordination sites, Raman spectra were measured. Raman bands due to the stretching vibration of an azo group in the various organic and complex compounds are known to appear in the 1200–1700 cm^{-1} region [18]. Namely, the Raman spectroscopy provides direct information [8,9] on whether or not an N atom in the azo group coordinates to Cu^{II} by comparing the stretching vibration bands borrowing from the azo groups in both free mtaq and the Cu^{II}-mtaq complexes.

As can be seen from Fig. 2, the spectrum of free mtaq at $-\log[H^+]$ 11.2_8 [(a), species mtaq^{2-}] shows bands (indicated by asterisk) at 1359 and 1400 cm^{-1} [18]. Upon the complexation of Cu^{II} with mtaq at $-\log[H^+]$ 2.5_8 (b), the complex Cu^{II}-mtaq has the bands at 1346 and 1391 cm^{-1}, which are situated at somewhat lower frequency position compared with those of free mtaq. Although the frequency difference between spectra (a) and (b) amounts to *ca* 10 cm^{-1}, these slight shifts towards lower frequency region are already known to be characteristic in the chelate-ring formation by using one of the N atom in the azo group [8,9]. On the other hand, the complex Cu^{II}-mtaq at $-\log[H^+]$ 7.2_6 (c) shows the bands at 1366 and 1402 cm^{-1}. These observations of band shifts toward higher frequency region are established as the result of no participation of the N atom in the azo group in metal complexes [8,9].

The validity of the above interpretation would be supported evidently by the comparison of Raman bands of mαtan which should coordinate deservedly to Cu^{II} with the S,N,O-site, as speculating by the molecular structure (Scheme 1). Namely, the bands of free mαtan (d) at 1327, 1363, and 1406 cm^{-1} shifted toward lower frequency region by complexation with Cu^{II} (e) at the S,N,O-site at 1318, 1346, and 1368 cm^{-1}, respectively.

Complexing equilibria and stability constants

The absorption spectral changes for the Cu^{II}-mtaq complexes due to the $-\log[H^+]$ variation are shown in Fig. 3. There are two distinct equilibria according to the $-\log[H^+]$ ranges studied. It can be seen from Fig. 3 that these spectral changes have clear isosbestic points at 20.2×10^3, 24.0×10^3 and 26.3×10^3 cm^{-1} in the lower $-\log[H^+]$ region (0–2.7_5), and at 21.0×10^3 and 25.4×10^3 cm^{-1} in the higher $-\log[H^+]$ region (2.7_5–5.8_9), respectively. That is, there are two types of equilibria in the Cu^{II}-mtaq complexation due to the $-\log[H^+]$ ranges studied.

All of the compositions of the complexes were determined by the continuous variation method. A sharp and single maximum at the ligand (or metal) mole fraction of 0.5 was obtained in all the Cu^{II}-mtaq sets in both lower and higher $-\log[H^+]$ ranges and the set of Cu^{II}-mαtan.

Judging from the protonation constants of mtaq in the lower $-\log[H^+]$ region, complexation equilibrium related to H_2mtaq at $-\log[H^+]$ 0–2.7_5 can be shown as follows:

$$Cu^{2+} + H_2\text{mtaq} \Leftrightarrow Cu(Hmtaq)^+\text{-S,N,O} + H^+.$$

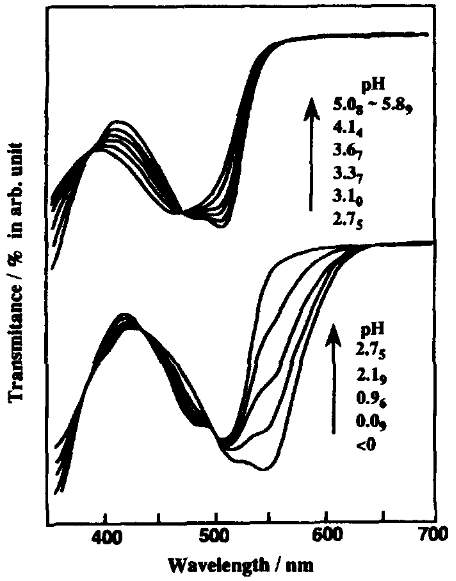

Fig. 3. Resonance Raman spectra of the free ligands and their Cu^{II} complexes: (a) mtaq^{2-} at $-\log[H^+] = 11.2_8$; (b) Cu(Hmtaq)$^+$-S,N,O at $-\log[H^+]$ 2.5_8; (c) Cu(mtaq)-N,O at $-\log[H^+] = 7.2_6$; (d) mαtan^{2-} at $-\log[H^+] = 10.2_8$; (e) Cu(mαtan)-N,O at $-\log[H^+] = 7.3_7$. [ligand] = [Cu^{II}] = 2.00×10^{-4} mol dm^{-3}, $\mu = 10^{-1}$ mol dm^{-3} NaClO$_4$, 25.0 ± 0.5°C.

It should be necessary for a discussion of the stability constants and kinetic consideration to take into account such species as $[Cu(OH)(H_2O)_5]^+$ besides $[Cu(H_2O)_6]^{2+}$ (hereafter, abbreviated as CuOH$^+$ for the former and Cu^{2+} for the latter, respectively). The stability constant $\beta_{Cu(Hmtaq)\text{-}S,N,O}$, corrected by side-reactions with CuOH$^+$ species ($K_{CuOH} = [CuOH^+][H^+]/[Cu^{2+}] = 10^{-8.0}$ [17]), because copper(II) usually forms a monohydroxo complex, and protonations of ligand, is calculated by equation (1):

$$\begin{aligned}
&\log \beta_{Cu(Hmtaq)\text{-}S,N,O} \\
&\quad = \log([Cu(Hmtaq)^+\text{-}S,N,O]/[Cu^{2+}][Hmtaq^-]) \\
&\quad = \log([Cu(Hmtaq)^+\text{-}S,N,O]/[H_2mtaq]) \\
&\quad + \log[H^+] - \log[Cu^{2+}] + \log K_{(hqNH)} + \log(\alpha_{Cu}\alpha_L),
\end{aligned} \tag{1}$$

where [Cu^{2+}] refers to experimental concentration (all the mixtures are composed of $[Cu^{2+}] \gg$ [ligand]), α_{Cu} is the side-reaction coefficient ($= 1 + K_{CuOH}/[H^+] \approx 1$) and $\alpha_L = (1 + K_{(hqNH)}K_{(hqOH)}[H^+]^2 + K_{(hqOH)}[H^+] = 5.84 \times 10^7)$, respectively, at $[H^+] = 10^{-1.50}$, where $\log[Cu(Hmtaq)^+\text{-}S,N,O]/[H_2mtaq] = 0$. Finally corrected stability constant is listed in Table 1.

In the $-\log[H^+]$ 2.7_5–5.8_9 region, a proton is released from the S,N,O-complex to give an N,O-complex as follows:

$$Cu(Hmtaq)^+\text{-}S,N,O \Leftrightarrow Cu(mtaq)\text{-}N,O + H^+.$$

The stability constant of the N,O-complex is obtained from equation (2).

$$\begin{aligned}
&\log \beta_{Cu(mtaq)\text{-}N,O} \\
&\quad = \log([Cu(mtaq)\text{-}N,O]/[Cu^{2+}][mtaq^{2-}]) \\
&\quad = \log([Cu(mtaq)\text{-}N,O]/[Cu(Hmtaq)^+\text{-}S,N,O]) \\
&\quad + \log[H^+] + \log \beta_{Cu(Hmtaq)\text{-}S,N,O} \\
&\quad + \log K_{(hqOH)} + \log(\alpha_{Cu}\alpha_L).
\end{aligned} \tag{2}$$

With the same treatment in the lower $-\log[H^+]$ region, the final corrected stability constant is listed in Table 1, together with that for Cu^{II}-mα tan complex.

Kinetics of complexations

The kinetics for the Cu^{II} complexations were studied under pseudo-first-order kinetic conditions with respect to Cu^{II} concentration using the relation between a logarithmic absorbance change and time t as in equation (3):

$$\ln[(A_i - A_\infty)/(A_t - A_\infty)] = k_{obs}t, \tag{3}$$

where A_i, A_t and A_∞ refer to the absorbance at the initial state, at time t and at the infinite equilibrium state of kinetic process, respectively. The rate constant $k_{obs(low)}$ of the Cu^{II}-S,N,O complexation process at a lower $-\log[H^+]$ range and $k_{obs(high)}$ for the Cu^{II}-N,O complexation process at higher $-\log[H^+]$ region were calculated separately, because of different equilibration processes. It was found that k_{obs} in each reaction process depends on the Cu^{II} concentration, thus showing pseudo-first-order kinetics.

By taking into consideration the protonation constants of mtaq, the hydrolysis constant of Cu^{II} and the stability constants of the 1:1 complexes, the formations of the Cu^{II}-S,N,O between $-\log[H^+]$ 0–2.7_5 and Cu^{II}-N,O complexes in the region of $-\log[H^+]$ 2.7_5–5.8_9 are considered to proceed as shown in Scheme 2.

In the case of the Cu^{II}-S,N,O complexation, four possible reaction pathways are proposed here, with their rate equations by using the steady-state approximation:

$$\begin{aligned}
&d[Cu(Hmtaq)^+\text{-}S,N,O]/dt \\
&\quad = [Cu^{2+}]\{(k_2[H_2mtaq] + k_1[Hmtaq^-]) \\
&\quad + [CuOH^+](k'_2[H_2mtaq] + k'_1[Hmtaq^-])\} \\
&\quad - [Cu(Hmtaq)^+\text{-}S,N,O]\{k_{-2}[H]^+ \\
&\quad + (k_{-1} + k'_{-2}) + k'_{-1}[OH^-]\}.
\end{aligned} \tag{4}$$

Here, k_i and k'_i denote the rate constants for the forward reactions concerning [Cu^{2+}] and [Cu(Hmtaq)$^+$-S,N,O], and k_{-i} and k'_{-i} those for the corresponding backward reactions, respectively. In this case, the protolytic processes were assumed to be always at equi-

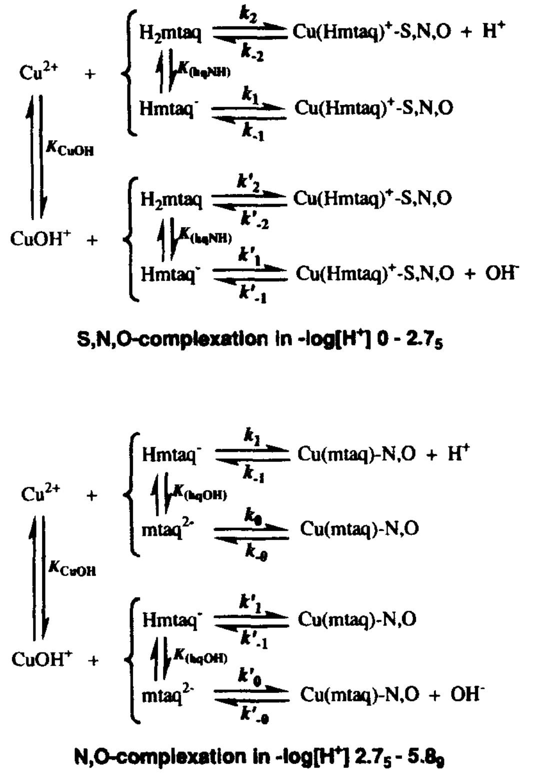

Scheme 2. Possible pathways of Cu^{II}-mtaq complexations at the S,N,O,-site in the lower $-\log[H^+]$ region and the N,O-site in the higher $-\log[H^+]$ region.

librium [19]. Under the pseudo-first-order kinetic conditions with respect to the Cu^{II} concentration, the forward rate constant can therefore be obtained from the experimental relation of $k'_{obs(low)}$ as a function of $[H^+]$ as equations (5) [11,12]:

$$k'_{obs(low)} = k_2 K_{(hqNH)}[H^+] + (k_1 + k'_2 K_{(hqNH)} K_{CuOH}) + k'_1 K_{CuOH}[H^+]^{-1}, \qquad (5)$$

where $k'_{obs(low)}$ relates k_{obs} obtained experimentally from equation (3), as in equation (6):

$$k'_{obs(low)} \equiv k_{obs(low)}/\{1/\beta_{Cu(Hmtaq)\text{-}S,N,O} + C_{Cu}/(K_{(hqNH)}[H^+]+1)(1+K_{CuOH}/[H^+])\}, \qquad (6)$$

where C_{Cu} corresponds to an experimental Cu^{II} concentration $(=[Cu^{2+}]+[Cu(Hmtaq)^+\text{-}S,N,O]+[CuOH^+])$. Figure 4(a) indicates that a linear relation apparently holds between the modified rate constant, $k'_{obs(low)}$, and $[H^+]$ with a significant intercept.

Likewise, the observed rate constant for the Cu(mtaq)-N,O complexation in the $-\log[H^+]$ 2.7_5–5.0_8 region, $k'_{obs(high)}$, can be related to $[H^+]$ as in equation (7) by using the pathways in Scheme 2 [11,12]:

$$k'_{obs(high)} = k_1 K_{(hqOH)}[H^+] + (k_0 + k'_1 K_{(hqOH)} K_{CuOH}) + k'_0 K_{CuOH}[H^+]^{-1}. \qquad (7)$$

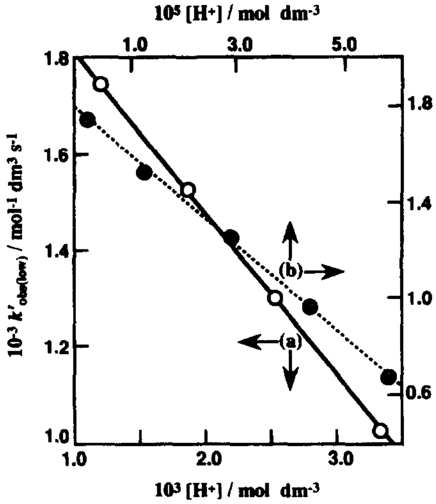

Fig. 4. Plots of (a) $k'_{obs(low)}$ and (b) $k'_{obs(high)}$ vs $[H^+]$ of Cu^{II}-mtaq complexes. $[Cu^{II}] = 2.00\times10^{-4}$ mol dm^{-3}, $[mtaq] = 2.00\times10^{-5}$ mol dm^{-3}, absorbance at 500 nm. $\mu = 10^{-1}$ mol dm^{-3} $NaClO_4$, 25.0 ± 0.2 C.

As can be seen from Fig. 4(b), it was found that the experimental data plots of $k'_{obs(high)}$ are proportional only to the $[H^+]$ term with a significant intercept.

In the lower $-\log[H^+]$ region, the formation of the matq complex proceeds through the reactions of $[Cu(H_2O)_6]^{2+}$ with H_2mtaq (k_2, from the slope) and $Hmtaq^-$ (k_1, from the intercept) and those of $[Cu(OH)(H_2O)_5]^+$ with H_2mtaq (k'_2, from the intercept) to give the complex $Cu(Hmatq)^+$-S,N,O. Likewise, in the higher $-\log[H^+]$ region, the complexation occurs *via* the pathways of $[Cu(H_2O)_6]^{2+}$ with $Hmtaq^-$ (k_1, from the slope) and $mtaq^{2-}$ (k_0, from the intercept) and those of $[Cu(OH)(H_2O)_5]^+$ with $Hmtaq^-$ (k'_1, from the intercept) to yield the complex Cu(matq)-N,O.

For comparison, a modified rate constant, $k'_{obs(m\alpha tan)}$, of the reaction between Cu^{II} and mαtan to give the complex $Cu(m\alpha tan)^+$-S,N,O was also measured. Although the relation of $k'_{obs(m\alpha tan)}$ with $[H^+]$ was not illustrated here, it was evident that the reaction proceeds mainly as $[Cu(H_2O)_6]^{2+} + Hm\alpha tan^- \rightarrow Cu(m\alpha tan)^+$-S,N,O($k$). The obtained kinetic parameters are summarized in Table 2.

The rate constant, k_2, for the Cu^{II}-mtaq set in the low $-\log[H^+]$ region was almost the same with that (k) of the Cu^{II}-mαtan set in magnitude. This may be a reflection of a same sterical environment to form both Cu^{II}-S,N,O complexes. In the reaction between Cu^{II} and mtaq, the rate constant k_2 in the lower $-\log[H^+]$ range is larger (10^2 order) than k_1 in the higher $-\log[H^+]$ region. This may be explained by a requirement of longer time to break the Cu^{II}—S bond in $Cu(Hmtaq)^+$-S,N,O to form the Cu(mtaq)-N,O complex.

Table 2. Kinetic parameters at $\mu = 10^{-1}$ mol dm^{-3} (KNO_3), 25.0 ± 0.2°C

	Rate constant (mol^{-1} dm^3 s^{-1})	Remark
$[Cu(H_2O)_6]^{2+} + H_2mtaq$	$k_2 = (3.2 \pm 0.5) \times 10^2$	Lower $-\log[H^+]$ region
$[Cu(H_2O)_6]^{2+} + Hmtaq^-$ (k_1) $[Cu(OH)(H_2O)_5]^+ + H_2mtaq$ (k'_2)	$(k_1 + k'_2 K_{(hqNH)} K_{CuOH}) = (2.2 \pm 0.4) \times 10^3$	Lower $-\log[H^+]$ region
$[Cu(H_2O)_6]^{2+} + Hmtaq$	$k_1 = (5.7 \pm 0.4) \times 10^0$	Higher $-\log[H^+]$ region
$[Cu(H_2O)_6]^{2+} + mtaq^{2-}$ (k_0) $[Cu(OH)(H_2O)_5]^+ + Hmtaq^-$ (k'_1)	$(k_0 + k'_1 K_{(hqOH)} K_{CuOH}) = (1.8 \pm 0.3) \times 10^4$	Higher $-\log[H^+]$ region
$[Cu(H_2O)_6]^{2+} + Hm\alpha tan^-$	$k = (4.1 \pm 0.5) \times 10^2$	$Cu(m\alpha tan)^+$-S,N,O

REFERENCES

1. Huang, H., Chikushi, H., Nakamura, M. and Kai, F., *Bull. Chem. Soc. Jpn*, 1990, **63,** 1985.
2. Huang, H., Asai, Y., Hirohata, M., Nakamura, M. and Kai, F., *Nippon Kagaku Kaishi*, 1990, 1348.
3. Huang, H., Kai, F., Asai, Y., Hirohata, M. and Nakamura, M., *Chem. Lett.*, 1991, 65.
4. Huang, H., Kai, F., Uragami, C., Hirohata, M., Chikushi, H., Yanaka, H., Honda, M. and Nakamura, M., *Bull. Chem. Soc. Jpn*, 1991, **64,** 1982.
5. Huang, H., Kai, F., Asai, Y., Hirohata, M. and Nakamura, M., *Bull. Chem. Soc. Jpn*, 1991, **64,** 2464.
6. Huang, H., Kai, F., Asai, Y., Hirohata, M. and Nakamura, M., *J. Coord. Chem.*, 1992, **25,** 357.
7. Huang, H., Kai, F., Shoda, T. and Nakamura, M., *J. Coord. Chem.*, 1993, **28,** 155.
8. Huang, H., Kai, F., Hirohata, M., Nakamura, M., Matsuzaki, S., Komori, K. and Tsunematsu, Y., *J. Coord. Chem.*, 1993, **30,** 131.
9. Hirohata, M., Kai, F., Kurosawa, K., Huang, H., Ishii, K., Matsuoka, Y., Komori, K. and Nakamura, M., *J. Coord. Chem.*, 1993, **30,** 379.
10. Hirohata, M., Kai, F., Piao, L., Komori, K., Matsuoka, Y. and Huang, H., *J. Coord. Chem.*, 1994, **31,** 237.
11. Piao, L., Kai, F., Hirohata, M., Matsuoka, Y. and Huang, H. *Polyhedron*, 1996, **15,** 3107.
12. Piao, L., Kai, F. and Hirohata, M., *Polyhedron*, 1997, **16,** 363.
13. Newton, W. E., *Sulfur, Its Significance for Chemistry, for the Geo-, Bio- and Cosmosphere and Technology*, ed. A. Muller and B. Krebs. Elsevier, Amsterdam, 1984, pp. 407–478.
14. Kielland, J., *J. Am. Chem. Soc.*, 1937, **59,** 1675.
15. Gerson, F. and Heibronner, E., *Helv. Chim. Acta*, 1962, **45,** 42; Hart, J. P. and Smyth, W. F., *Spectrochim. Acta*, 1980, **A36,** 279.
16. Srivastava, S. L. and Prasad, M., *Spectrochim. Acta*, 1984, **A40,** 681; Mason, J., Sarawat, B. S. and Mehrotra, R. C., *Polyhedron*, 1985, **4,** 2089; Lang, L., *Absorption Spectra in the Ultraviolet and Visible Region*. Publishing House of the Hungarian Acad. Sci., Budapest, 1959.
17. Sillén, L. G. and Martell, A. E., *Stability Constants of Metal-Ion Complexes*. The Chemical Society, London, 1964.
18. Brandmüller, J., Hacker, H. and Schrötter, H. W., *Chem. Ber.*, 1966, **99,** 765.
19. Eigen, M., *Pure Appl. Chem.*, 1963, **6,** 97.